PhD Thesis

Structural studies and tissue distribution of human GCPII and characterization of its rat and porcine orthologs

By Miroslava Rovenská

Supervisor: Jan Konvalinka, PhD

Department of Biochemistry
Faculty of Science
Charles University

Institute of Organic Chemistry and Biochemistry
Gilead Sciences & IOCB Research Centre
Academy of Sciences of the Czech Republic

Prague 2008

ACKNOWLEDGEMENTS

Here I would like to thank all the people who enabled me to work on this thesis and made it pleasant to me. First, I would like to thank all the members of the department I was working at, particularly my supervisor Jan Konvalinka who has accepted me on board. My special thanks belong to the members of the „NAALADase team“ who supplied me with valuable advice and optimism that I was losing during all the unsuccessful experiments: Peťucha for loyalty, empathy, and for alliance in fighting with a confounded project, Pavlik for being the most gentle data bank, Bimča for the coffee breaks and for always having the top view, Káki for collaboration and inspiration, Honzík for giving me the optimism lessons, Tom for not giving up and not hating me despite my excellent proposal of his bachelor project, and Tvrďák for not keeping the top sportsman’s regime all the time. I thank all the people of the „HIV“ and „racemase“ teams for contributing to the excellent atmosphere at our workplace. I thank also all the former members of our group who are now abroad but awaiting all the time, especially Cyril Bařinka, the best guitar player and, in addition, leading person of the GCPII crystallization studies, and Jana Václavíková for making my starts at the IOCB so funny.

I thank all my friends from outside the lab walls, too, for every moment that we spent together since it always turned my mood for the better and thus enabled me to try again.

Last but not least, I thank my family not only for supporting me during all my studies but also for being here.

CONTENTS

1 PREFACE

Glutamate carboxypeptidase II (GCPII) is a membrane-bound metallopeptidase of great pharmacological importance.

It acts as a peptidase in the nervous system, where it cleaves the most abundant peptide neurotransmitter, N-acetyl-L-aspartyl-L-glutamate (NAAG), and releases glutamate into a synaptic cleft. Inhibition of this NAAG-hydrolyzing activity has been shown to be neuroprotective in neurological disorders caused by excessive glutamate transmission, such as stroke or neuropathic pain.

GCPII is also used as a marker of prostate cancer, since its expression is increased in malignant prostate tissue. GCPII expression emerges in tumor-associated neovasculature; therefore, GCPII is believed to be a potential target for anti-tumor therapy.

GCPII implications in such diagnostic and therapeutic strategies are being actively pursued. In this context, analysis of the GCPII active site and events occurring upon ligand binding is necessary in order to design novel inhibitors/substrates with a higher affinity to GCPII and better pharmacokinetic parameters. Moreover, a suitable animal model which displays similar kinetic parameters and tissue distribution of the corresponding GCPII ortholog is needed for *in vitro* and *in vivo* studies.

The thesis presents several new findings in these fields. Papers concerning the mechanism of ligand binding in the GCPII active site and analyzing rat and pig GCPII orthologs and their tissue distribution are included. These findings might help to design and develop new therapeutic and/or diagnostic approaches.

2 ABBREVIATIONS

2-MPPA	(2-(3-mercaptopropyl)pentanedioic acid
2-PMPA	2-(phosphonomethyl)pentanedioic acid
β-NAAG	N-acetyl-β-L-aspartyl-L-glutamate
Ac	Acetyl
ALS	Amyotrophic lateral sclerosis
AMPA	Amino-3-hydroxy-5-methylisoxazole-4-propionic acid
BPH	Benign prostatic hypertrophy
CNS	Central nervous system
DTT	Dithiothreitol
EDTA	Ethylenediaminetetraacetic acid
EGTA	Ethyleneglycol-bis(2-aminoethylether)-N,N,N′,N′-tetraacetic acid
FDA	Food and Drug Administration
GABA	γ-Aminobutyric acid
GCPII	Glutamate Carboxypeptidase II
GCPIII	Glutamate Carboxypeptidase III
hGCPII (≡ rhGCPII)	Recombinant extracellular part of human GCPII
LNCaP cells	Cell line derived from prostate cancer metastasized to lymph node
L-SOS	L-serine-O-sulfate
MCAO	Middle Cerebral Artery Occlusion
mGluR	Metabotropic glutamate receptor
MHC	Major Histocompatibility Complex
NAA	N-acetyl-L-aspartate
NAAG	N-acetyl-L-aspartyl-L-glutamate
NMDA	N-methyl-D-aspartate
PC3	prostate cancer cell line
pGCPII	Recombinant extracellular part of porcine GCPII
PSM’	Truncated form of prostate-specific membrane antigen
PSMA	Prostate-specific Membrane Antigen
PSMA-L	PSMA-like gene
QA	Quisqualic acid
rGCPII	Recombinant extracellular part of rat GCPII

rhGCPII (≡ hGCPII)	Recombinant extracellular part of human GCPII
SDS PAGE	Sodium dodecyl sulfate electrophoresis in polyacrylamide gel
TGF-β	Transforming growth factors-β

3 INTRODUCTION

3.1 GCPII discovery

In 1987, Robinson *et al.* identified a novel N-acetylated-alpha-linked acidic dipeptidase activity in rat brain membranes, cleaving the most abundant peptide neurotransmitter N-acetyl-L-aspartyl-L-glutamate (NAAG) into N-acetyl-L-aspartate and L-glutamate. They named the corresponding enzyme NAALAdipeptidase (N-acetylated alpha-linked acidic dipeptidase), which was later abbreviated to NAALADase [1].

In the same year, Horoszewicz *et al.* obtained a new monoclonal antibody termed 7E11-C5 following immunization with LNCaP cells, isolated from a human prostate cancer. This antibody was shown to react with human prostatic epithelium, both normal and malignant, but did not recognize any of the 26 various nonprostatic tumors and the majority of 28 normal organs tested; positive staining occurred only in a few samples of normal kidneys [2]. Since the antigen of this antibody was thought to be prostate-specific, it was called prostate-specific membrane glycoprotein, later prostate-specific membrane antigen (PSMA).

In 1996, it was found that PSMA is capable of NAAG hydrolysis yielding N-acetyl-aspartate and glutamate and displays high sequence identity to NAALADase [3]. Thus, it was found that these two distinct names actually refer to one protein. Moreover, in the same year, Pinto *et al.* reported another activity of this enzyme: folate hydrolase activity [4], which is believed to participate in folate absorption in small intestine [5; 6].

To make the situation clearer, PSMA/NAALADase/folate hydrolase was given the unified name glutamate carboxypeptidase II (GCPII; EC 3.4.17.21), approved by IUBMB. This name I am going to prefer throughout the whole text, with the occasional exception for the case of clinical implications, especially those concerning prostate cancer, where the term PSMA is frequently used.

3.2 Human GCPII - gene

The human GCPII gene consists of 19 exons and 18 introns spanning approximately 60 kbp of genomic DNA. Based on the sequence, GCPII was predicted to be a type II integral

membrane protein, which is in agreement with the finding that a portion of the coding region from nucleotide 1250 to 1700 has 54% homology to the human transferrin receptor mRNA [7; 8]. The gene encoding for GCPII was mapped to chromosome 11p11.2 [9].

3.3 Human GCPII - protein

Full-length (2.65 kbp) cDNA encoding GCPII was cloned. The corresponding protein was predicted to be 750 amino acids long, with a molecular mass of 84 kDa. Amino acids 20-43 were deduced to form a transmembrane domain; the major portion of the protein was shown to be C-terminal to the transmembrane domain and contain several potential N-glycosylation sites [8]. Coupled in vitro transcription/translation of the full-length GCPII cDNA indeed yielded an 84-kDa protein. Posttranslational modification of this protein with pancreatic canine microsomes provided GCPII of the expected molecular mass of 100 kDa [10].

Ten N-glycosylation sites were found in GCPII expressed in S2 cells; most of the glycosylations were shown to be indispensable for the enzymatic activity of GCPII. Inhibition of N-glycosylation also blocked the secretion of the recombinant protein to the S2 cell media [11].

The cytoplasmic tail of GCPII contains the dileucine motif, which has been shown to function as internalization signal [12]. Consistently with this finding, GCPII internalization via clathrin-coated pits was observed [13], suggesting the possibility of GCPII acting as a receptor for an unknown ligand. This speculation is further supported by the finding that the cytoplasmic domain of GCPII interacts with filamin A, actin cross-linking protein, and that this association modulates the rate of GCPII internalization [14].

Recombinant extracellular domain of GCPII as well as full-length GCPII in LNCaP lyzate were shown to form a dimer under native conditions and it was the dimer that exhibited folate hydrolase as well as NAALADase activity (contrary to monomer) [15]. Nevertheless, this observation has not been independently confirmed yet.

GCPII amino acid sequence is depicted in Fig. 1.

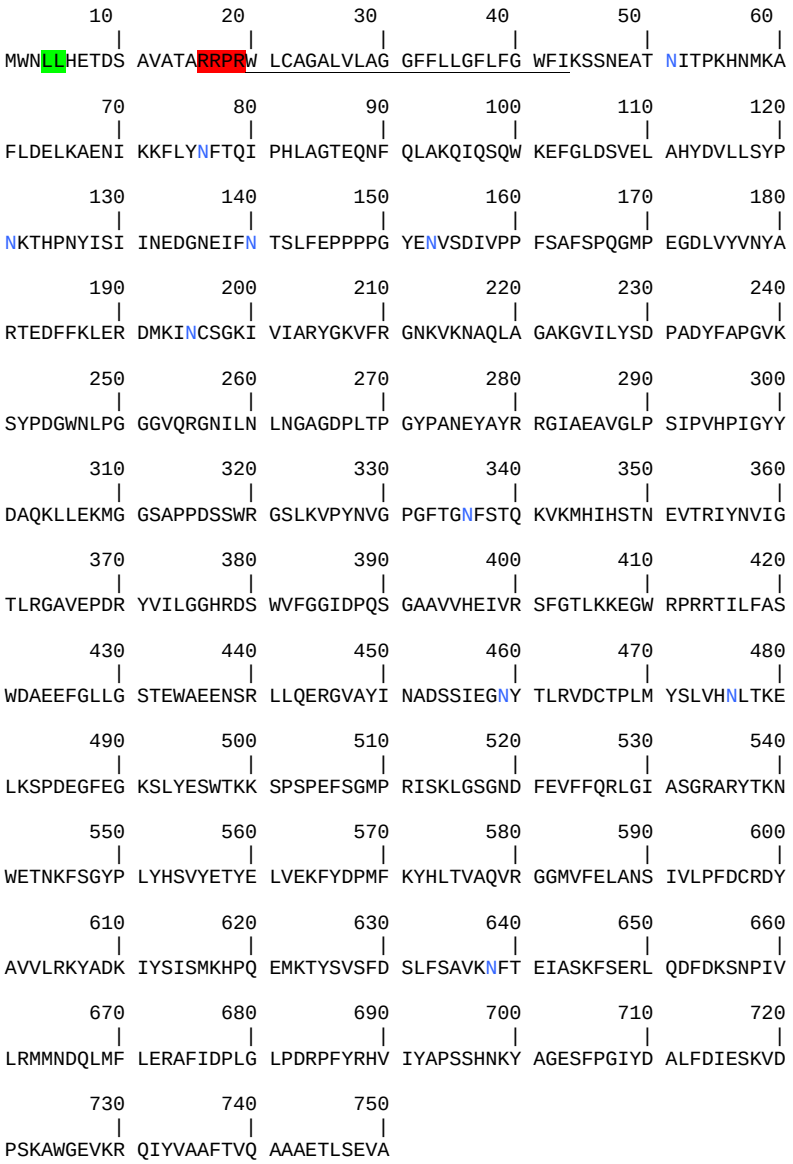

Fig. 1: Amino acid sequence of human GCPII. The dileucine signal is shaded green, the positively charged arginine anchor is shaded red, and the transmembrane domain is underlined. "N" in blue indicates N-glycosylation site.

3.4 Structure of human GCPII

3.4.1 Predictions

Based on the homology of GCPII with transferrin receptor, Rawlings and Barrett predicted the domain structure of GCPII in 1997. They also assigned its catalytic domain to

the metallopeptidase family M28; using the known structure of the *Vibrio proteolyticus* aminopeptidase of this family, they predicted that the GCPII amino acids His377, Asp387, Glu425, Asp453, and His553 are the ligands of two zinc atoms bound in the active site [16]. The predicted structure of GCPII consisted of six domains: domain A forming a short N-terminal cytoplasmatic tail (amino acids 1-18), hydrophobic transmembrane domain B (amino acids 19-43), and four extracellular domains: C (amino acids 44-144), D (amino acids 173-249), E (amino acids 274-586), and F (amino acids 587-750), of which domain E was the catalytic one. Two proline and glycine rich regions (145-172 and 249-273) are claimed to be linker peptides between the domains.

Glu424 was predicted to act as a proton shuttle in the catalytic mechanism (see below) [17].

3.4.2 Crystal structures

3.4.2.1 Overall structure

The first crystal structure of the extracellular part of human GCPII was published in 2005 (at the resolution of 3.5 Å) and revealed a symmetric homodimer with structural similarity to transferrin receptor [18]. Unlike transferrin receptor, there is a protease domain in the structure of GCPII containing a binuclear zinc site, catalytic residues, and a proposed substrate-binding arginine patch. Each monomer consists of a protease domain (residues 56–116 and 352–591), an apical domain (residues 117–351), and a helical domain (residues 592–750). A large cavity at the interface between the three domains includes a binuclear zinc site, which, together with the conservation of many of the cavity-forming residues among GCPII homologs, identifies this cavity as the substrate-binding site. Amino acids from all three domains are involved in substrate binding. Seven of the glycosylation sites show carbohydrate electron density; carbohydrates attached to Asn638 are positioned such that they could be involved in intersubunit interactions.

In 2006, the structure of the extracellular portion of human GCPII (residues 44–750) in complex with its inhibitor GPI-18431 (Fig. 2) and with glutamate, the product of substrate cleavage, was published, in both cases acquired at much better resolution than the previous structure [19].

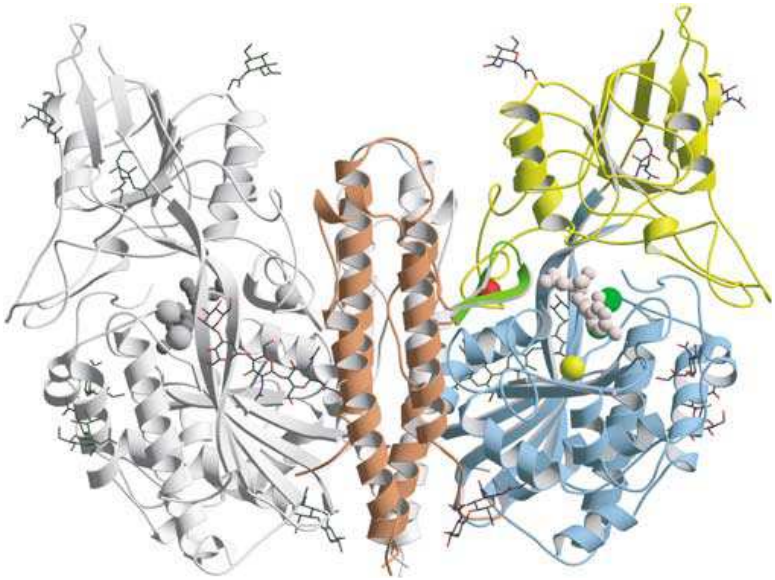

M E M B R A N E

Fig. 2: Three-dimensional structure of the GCPII dimer. One subunit is shown in gray, while the other is colored according to organization into domains: protease domain blue, apical domain yellow, C-terminal (helical) domain brown. The dinuclear zinc cluster at the active site is indicated by dark green spheres, Ca^{2+} ion by a red sphere, and the Cl^- ion by a yellow sphere. The GPI-18431 inhibitor is shown as small beige balls. The "glutarate sensor" (see below) is shown in light green. The seven carbohydrate side chains located in the electron density maps are indicated. Taken from [19].

3.4.2.2 Coordination of zinc ions

The zinc ions are each coordinated by three endogenous ligands: histidine (His553 or His377), aspartate (Asp453) or glutamate (Glu425), and a bridging aspartate (Asp387). Additionally, a water molecule asymmetrically bridges the zinc ions (Fig. 3).

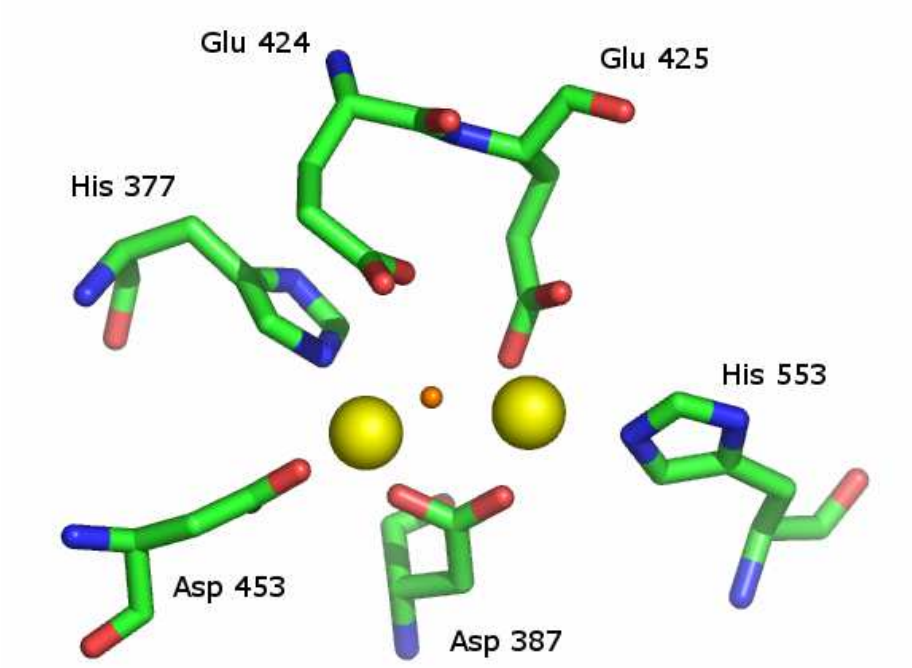

Fig. 3: Active site of GCPII and zinc ions coordination. Zn^{2+} ions (yellow spheres) are coordinated by Asp453, His377, Glu425, His553, and Asp387. Glu424, acting as a proton shuttle, is also shown, as well as the water molecule bound during hydrolysis (small orange sphere). Nitrogen atoms are colored blue, oxygen atoms red. The picture was generated using PyMOL and the structure of the extracellular part of human GCPII complexed with glutamate (acquired by Cyril Bařinka) [19].

3.4.2.3 Substrate/inhibitor binding in detail

Using the high-resolution structures of the extracellular portion of human GCPII in complex with its inhibitor GPI-18431 and with the cleavage product glutamate, the ligand binding in the GCPII active site could be analyzed in detail [19].

The inhibitor GPI-18431 occupies the S1 and S1' substrate-binding sites of GCPII, whereas the product of the cleavage, L-glutamate, resides in the S1' pocket only. In both the complexes, the C-terminal α-carboxylate group is recognized by Arg210 through a strong ion pair and by hydrogen bonds from the hydroxyl groups of Tyr552 and Tyr700. The glutamate side chain is recognized by a salt bridge between the γ-carboxylate and Lys699 and also by a hydrogen bond with the side-chain amide of Asn257. The free amino group of L-glutamate makes interactions with the γ-carboxylate of Glu424, with the carbonyl oxygen of Gly518 and with a water molecule that is hydrogen-bonded to the hydroxyl group of Tyr552. Lys699 and

Tyr700 participate in forming the ‘glutarate sensor’ (amino acids 692-704) at the bottom of the S1’ pocket [19; 20] that probes the S1’ pocket for the presence of a glutarate moiety and realizes an induced-fit mechanism of substrate recognition. The S1’ pocket of GCPII is defined by residues Phe209, Arg210, Asn257, Gly427, Leu428, Gly518, Lys699 and Tyr700. The putative S1 pocket is defined by residues Ser454, Glu457, Asp465, Asn519, Gly548, Tyr549, and by a stack of three arginines (Arg463, Arg534, and Arg536) [20].

3.4.2.4 Chloride ion

At the ‘bottom’ of the S1 pocket, there is a chloride ion bound to Arg534, Arg580, Asp453, Asn451, and two water molecules [19]. Based on the structure of ligand-free GCPII, the Cl^- ion was suggested to play a role in stabilizing the invariant conformation of Arg534 and one of the two possible conformations of Arg536, and also in neutralizing the positive charge contributed by their guanidinium groups [20].

3.4.2.5 Dimerization interface and calcium ions

Dimerization interface of GCPII is comprised of C-terminal (helical) domain of one monomer and protease and apical domains of the other [19]. Bařinka *et al.* also located one calcium ion into the GCPII structure. The Ca^{2+} ion is too remote from the active site to be involved in the catalytic activity. More likely, its role is to hold protease and apical domains together through coordinative interactions. Furthermore, it is probably important for dimerization. Sugars at Asn638 were also shown to contribute to dimer formation.

3.5 GCPII as an enzyme

Hydrolytic function can be attributed to GCPII in the nervous system and small intestine; however, its role in other tissues with pronounced GCPII expression (mainly prostate and kidney) remains to be elucidated. We can speculate that GCPII acts not only as hydrolase; based on its similarity to transferrin receptor, capability to internalize and interaction with filamin A, GCPII is suspected of being a receptor for a yet unknown ligand.

3.5.1 GCPII as a peptidase

GCPII is a peptidase belonging to the M28 peptidase family, which contains cocatalytic zinc metallopeptidases [16]. The catalytic domain of GCPII has been identified by sequence similarities to low molecular weight aminopeptidases from *Streptomyces griseus* and *Vibrio proteolyticus* (also known as *Aeromonas proteolytica*), which also have a binuclear Zn^{2+} center at the active site with two zinc ions sharing a bridging carboxylate ligand [21; 22].

Based on GCPII similarity to these proteases, amino acids involved in zinc binding, adjacent amino acids and amino acids implicated in substrate binding were mutated and their influence on GCPII activity was tested. It was confirmed that the amino acids coordinating zinc ions (His377, Asp387, Glu425, Asp453, and His553) are indispensable for enzyme activity; great influence on enzyme activity was noticed also for mutations of Asp379, Pro388, Glu424, and Tyr552. Mutation of predicted substrate ligands was less disruptive; of these, Arg463, Asn519, Arg536, Thr538, and Lys545 were found to play role in substrate hydrolysis [17].

Another mutational study performed by Mlčochová *et al.* suggests that the amino acid residues delineating the S1' pocket of the enzyme (namely Arg210) contribute primarily to the high affinity binding of GCPII substrates/inhibitors, whereas the residues forming the S1 pocket might be more important for the 'fine-tuning' of GCPII substrate specificity. Within the S1' residues, Arg210, Asn257, Tyr552, Lys699, and Tyr700 were shown to play an important role in substrate binding; within the S1 pocket, the influence on substrate cleavage is mainly attributable to Asn519, Asp520, and Arg536 [23].

3.5.2 Reaction mechanism

Glu424 is the likely catalytic acid/base of GCPII catalyzed hydrolysis [17]. In the GCPII/glutamate complex, one of its carboxylate oxygens is hydrogen-bonded to the water molecule bridging the two zinc ions, whereas the other interacts with the free amino group of the bound glutamate, the cleavage product. This is in agreement with the function of Glu424 as a proton shuttle that abstracts a proton from the zinc-bound catalytic water and transfers it to the leaving amino moiety of glutamate. Activated through the initial proton abstraction, the catalytic water attacks the carbonyl group of the aspartyl residue of NAAG [19]. This

mechanism, which is derived from the crystal structure of GCPII in complex with glutamate, is very similar to what has been described for metalloproteinases such as thermolysin and carboxypeptidases [24].

3.5.3 NAAG cleavage parameters and optimum

Lysates of PC3 cells transfected with human GCPII display the K_m value of 150 nM for NAAG cleavage [25]. For purified GCPII, the K_m and k_{cat} values of NAAG cleavage were shown to depend on salt concentration and pH of the reaction buffer; in 20 mM NaCl and pH 7.4, the K_m of 1.2 µM and k_{cat} of 1.1 s^{-1} were measured for GCPII and NAAG. pH optimum for GCPII was found to lay between pH 8 and 9 [26].

3.5.4 NAAG and the role of GCPII in the nervous system

NAAG-hydrolyzing activity of GCPII was discovered in 1987 in rat brain [1]. In the adult rat nervous system, GCPII is predominantly expressed by astrocytes [27; 28]. GCPII is also expressed by non-myelinating Schwann cells in the rat peripheral nervous system [29]. In human, hippocampal astrocytes and also neurons were found to be GCPII-positive by immunochemistry staining [30; 31]. On the other hand, the study performed by Šácha *et al.* in human did not reveal GCPII positivity in other cell type of the CNS than astrocytes [32].

NAAG is the most abundant peptide neurotransmitter in the mammalian nervous system, reaching millimolar concentrations in brain and spinal cord [33]. Immunohistochemical studies demonstrated a broad distribution of this peptide throughout the mammalian brain, spinal cord, and sensory neurons [34; 35; 36]. NAAG has been identified in neurons that use a variety of neurotransmitters, including glutamate, GABA, serotonin, norepinephrine, dopamine, and acetylcholine [36; 37; 38].

GCPII, localized in membranes of astrocytes, hydrolyzes NAAG released to the synaptic cleft into N-acetyl-L-aspartate (NAA) and L-glutamate [1] (Fig. 4).

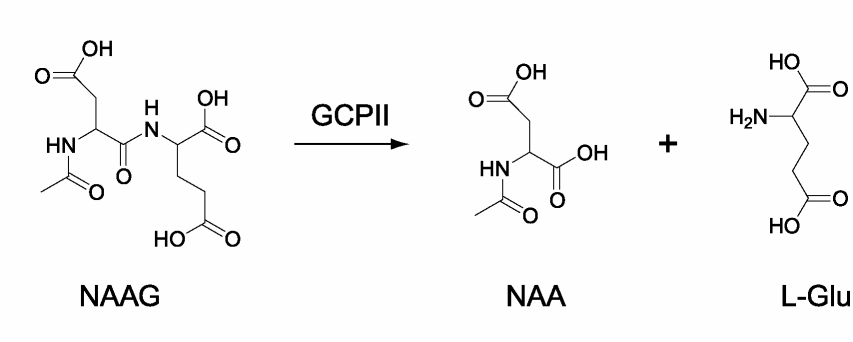

Fig. 4: NAAG cleavage catalyzed by GCPII releases N-acetyl-L-aspartate and free L-glutamate [1].

NAAG was found to act as a low-potency agonist at the NMDA (N-methyl-D-aspartate) receptors (but not kainate or AMPA receptors) on mouse spinal cord neurons in cell culture or expressed on *Xenopus* oocytes, although with a much lesser potency than glutamate [39; 40]. On the other hand, NAAG fails to mimic the excitatory response to NMDA in the cat dorsal lateral geniculate [41]. One possible explanation could be that NAAG has differential potency at various NMDA receptor subtypes. Also, given the lower effectiveness of NAAG in activating the NMDA conductance than in occupying the binding site, it also may compete with glutamate for the receptor. This may be responsible for the reports of an inhibitory effect of NAAG on NMDA-induced events [42; 43]. Thus, NAAG may act as a mixed agonist /antagonist at specific NMDA receptor subtypes.

Beside its action on the NMDA receptors, NAAG selectively and potently activates metabotropic glutamate receptors mGluR3 (of the group II) [44; 45]. Via reduction in cAMP or a direct action of G proteins on voltage-dependent calcium channels, activation of presynaptic mGluR3 by NAAG can suppress subsequent synaptic release. Consistently, Zhao *et al.* demonstrated that NAAG decreases GABA release in cortical neurons in cell culture via mGluR3, protein kinase A, and L-type calcium channels [46]. Importantly, it was found that NAAG inhibits glutamate release at mossy fiber-CA3 synapses through presynaptic activation of group II mGluRs [47].

Moreover, activation of mGluR3 on glial cells has a neuroprotective effect on neurons, since it leads to secretion of the transforming growth factors-β (TGF-β) by astrocytes [48; 49]. Overview of the NAAG action is depicted in Fig. 5.

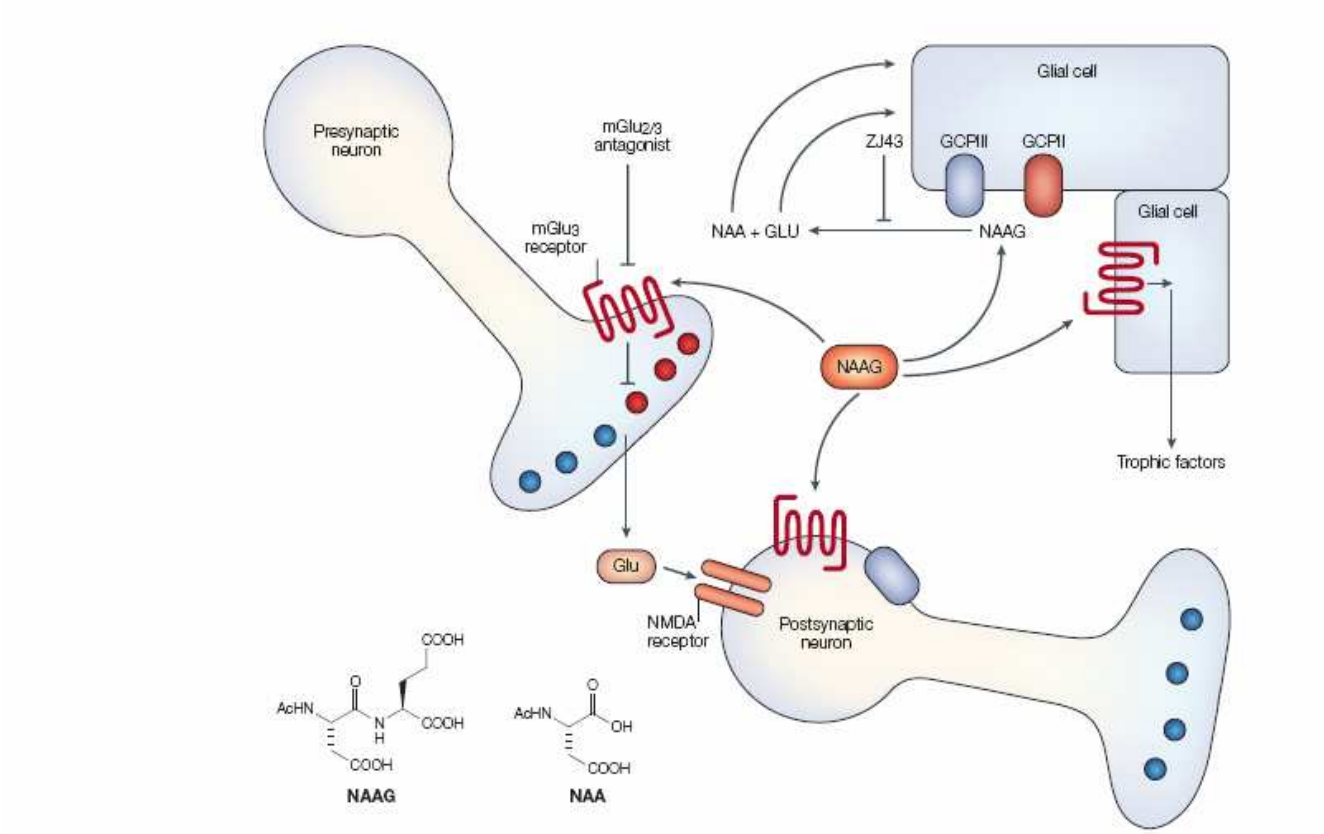

Fig. 5: NAAG action scheme. Glutamate carboxypeptidase II and III modulate glutamatergic neurotransmission by hydrolyzing NAAG in the extracellular space. NAAG is co-released with glutamate and upon very high neuron excitation reaches levels sufficient to dampen further release of glutamate. This is achieved by activation of the presynaptic mGluR3 receptors. Inhibition of GCPII and III results in elevated NAAG levels, increased activation of presynaptic mGluR3 and greater inhibition of Glu-mediated neurotransmission. NAAG also activates glial mGluR3 and thus stimulates the release of neuroprotective trophic factors. ZJ43, urea-based GCPII inhibitor. Taken from [50].

Since GCPII-catalyzed hydrolysis terminates NAAG action and simultaneously provides glutamate, it modulates the glutamatergic transmission. Thus, it might be involved in various neurological disorders associated with the dysregulated glutamate transmission (see the chapter “GCPII in Neuropathies”).

3.5.5 GCPII in small intestine

Folylpoly-γ-glutamates from food cannot be directly taken into the cells. Only after the removal of poly-γ-glutamates, released folic acid can be transported across the intestinal wall

by folate transporters. GCPII hydrolyzes dietary folates to allow their intestinal absorption [51; 4] (Fig. 6).

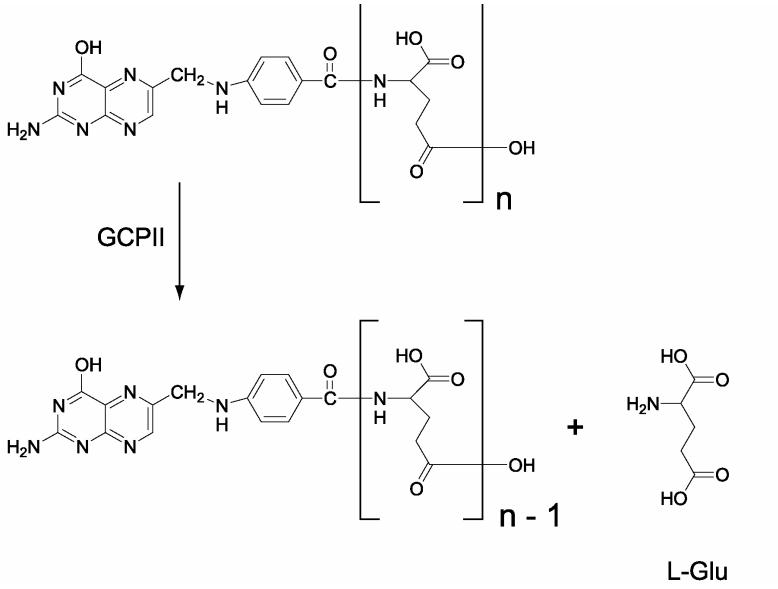

Fig. 6: In the small intestine, GCPII hydrolyzes dietary folates, cleaving off γ-linked glutamates from folylpoly-γ-glutamates (n=5-7).

3.5.6 GCPII inhibitors

In the Robinson's pilot study, EDTA, EGTA, and phosphate as chelating agents and DTT, iodoacetate, and bestatin were shown to inhibit GCPII in higher concentrations. Higher inhibition potency was discovered for glutamate (IC_{50}=31 µM), serine-O-sulfate (IC_{50}= 42 µM), and especially for quisqualic acid (Fig. 7; IC_{50}=0.48 µM, K_i value was determined to be 1.9 µM) [1; 52]. Later, β-NAAG (N-Ac-β-L-Asp-L-Glu) was found to inhibit GCPII with the K_i value of 0.7 µM (Fig. 7) [52].

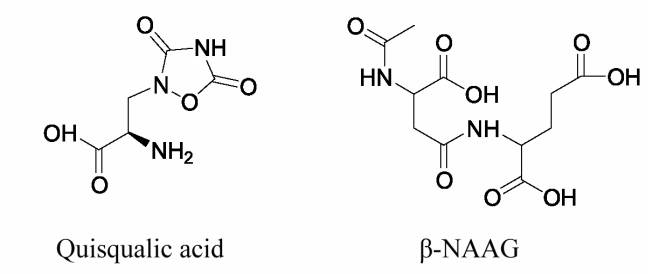

Fig. 7: GCPII inhibitors quisqualic acid and β-NAAG (N-Ac-β-L-Asp-L-Glu).

The first potent and selective inhibitor of GCPII, 2-(phosphonomethyl)pentanedioic acid (2-PMPA; Fig. 8), was designed and synthesized by Jackson *et al.* in 1996 and displays the K_i value of 0.3 nM [53]. Since then, many other phosphonate/phosphinate-based GCPII inhibitors were synthesized and tested [54; 55].

Subsequently, a phosphonate moiety was replaced by a thiol group; the resulting derivatives showed lower polarity accompanied by an increased *in vivo* efficacy. The thiol-based (2-(3-mercaptopropyl)pentanedioic acid (2-MPPA; Fig. 8) was the first reported orally active GCPII inhibitor, with the K_i value of 90 nM [56; reviewed in 50].

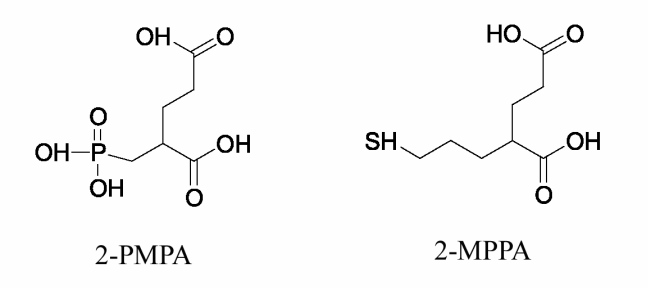

Fig. 8: GCPII inhibitors 2-PMPA, 2-(phosphonomethyl)pentanedioic acid, and 2-MPPA, (2-(3-mercaptopropyl)pentanedioic acid.

Based on the structures of 2-PMPA and 2-MPPA, the hydroxamate derivatives have been designed with the hydroxamate moiety alternating the phosphonate/phosphinate moiety as a zinc-binding group. However, they display only moderate to low inhibitory activity against GCPII (the most potent displays the IC_{50} value of 220 nM) [57].

In addition, urea-based inhibitors were synthesized, among them some with the K_i value in subnanomolar range [58; 59]. From this group of compounds, the PBDA inhibitor has been derived by replacing the central carbonyl group by a phosphinate moiety (Fig. 9). It acts not only as a potent GCPII inhibitor (EC_{50}=22 nM), but also exhibits good potency and selectivity as an agonist for mGluR3 receptors [60].

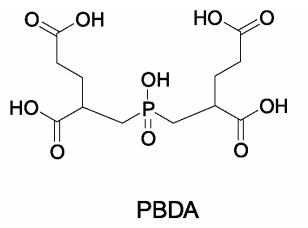

Fig. 9: Formula of GCPII inhibitor PBDA.

3.6 GCPII expression in human

Human brain, prostate, and kidney are considered to be the principal sites of the GCPII expression.

3.6.1 mRNA level

Ribonuclease protection analysis demonstrated that the principal site of the GCPII mRNA expression is the prostate. GCPII expression was found to be hormonally down-regulated by steroids in LNCaP cells [10]. Another study also confirmed the abundant GCPII mRNA expression in the prostate [61].

GCPII mRNA was detected also in human testis, epididymis, seminal vesicles, heart, brain, liver, lung, kidney, spleen, thyroid gland, colon, ovary, small intestine, and in the PC-3 and LNCaP prostatic cancer cell lines [62; 63; 64].

3.6.2 Protein level

Since performed by different methods and in various experimental set-ups, the attempts to study GCPII expression on protein level sometimes give contradictory results, which is particularly the case of GCPII detection in serum. Surprisingly, until recently only one group was able to detect GCPII protein in brain.

The pilot immunohistochemistry study performed by Horoszewicz *et al.* using the 7E11-C5.3 antibody demonstrated that the GCPII expression is restricted to the epithelium of localized and metastatic prostate cancer, benign prostatic hypertrophy, and normal prostate tissue. None of the 28 different normal organs was reactive except for a heterogeneous staining of some of the kidney samples [2]. However, since the 7E11-C5.3 antibody recognizes the N-terminal part of GCPII localized in cytosol, it could fail in visualizing GCPII in the membranes of viable cells.

Rochon *et al.* detected GCPII in serum - from prostate cancer patients as well as normal donors - and in seminal fluid of normal donors using this antibody [65]. On the other hand, the first study of the same group denied the presence of GCPII in sera of normal donors [2].

Another group could not detect GCPII in serum by Western blot analysis even in patients with actively progressive metastatic disease [66], while Xiao *et al.* documented increased levels of GCPII in sera of prostate cancer patients compared to normal donors [67].

Slight GCPII expression was found (using the 7E11-C5.3 antibody) in normal salivary gland and brain; higher amounts were detected in small intestine [66]. Positive immunohistochemistry staining using this antibody has also been noticed for proximal renal tubules, duodenal mucosa, and colon [68].

A dual-monoclonal sandwich assay (capturing of GCPII by a biotinylated antibody 7E11-C5.3 immobilized onto a streptavidin-coated microtiter plate, followed by detection of captured GCPII by an Eu-labeled antibody) found the highest levels of GCPII in the prostate; low levels were observed in membranes from ovary and breast, and negligible levels in membranes from skin, liver, intestine, and kidney [69].

An extensive immunohistochemical study recently revealed GCPII expression in the epithelium of prostate, urinary bladder, proximal tubules of kidney, liver, esophagus, stomach, small intestine, colon, breast, fallopian tubes and testicular seminiferous tubules, hippocampal neurons and astrocytes, ependyma, cortex and medulla of the adrenal gland, and ovary stroma [31]. In 2007, an abundant GCPII expression in various compartments of human brain was confirmed by the study performed by Šácha *et al.* [32].

3.6.3 GCPII expression in cancer

3.6.3.1 Prostate cancer

Normal as well as cancer prostate consistently exhibit a profound GCPII expression and so do most prostate cancer metastases (lymph node and bone) [2; 68; 70].

Sweat *et al.* found that the number of positively stained cells was lowest in benign epithelium; the corresponding number in cancer and lymph node metastases was similar and higher in both cases [70]. The greatest extent and intensity of PSMA staining was observed in the highest grades of prostate adenocarcinoma [71].

3.6.3.2 Other cancers

Although several groups did not detect GCPII expression in any other than prostate cancer [2; 68], later these findings had to be reconsidered. Both PSMA mRNA and protein were identified in normal and neoplastic renal tissue [72]. Later, it was shown that GCPII protein can be detected in neoplasm of the prostate, kidney, stomach, small intestine, colon, lung, and testis [31]. However, in 2007, an extensive study of more than 3000 samples analyzing GCPII expression in normal and corresponding neoplastic tissues demonstrated that despite GCPII expression by subsets of various types of malignancies, only prostate cancer samples consistently display GCPII positivity in high percentage of specimens [73].

3.6.3.3 Tumor neovasculature

Intense staining for PSMA was observed in endothelial cells of capillary vessels in some of renal carcinomas and with a lesser frequency in colon carcinomas [68]. Later, PSMA mRNA and protein expression were demonstrated in the endothelium of tumor-associated neovasculature of various solid malignancies (e.g. renal carcinoma, carcinoma of the urinary bladder, colonic adenocarcinoma, malignant melanoma, breast carcinoma) whereas no PSMA mRNA or protein expression was found in the vascular endothelial cells of the corresponding benign tissue samples [63; 74]. Therefore, it should be judged whether the observed GCPII positivity in particular malignancy specimens comes from the neoplastic tissue or endothelia.

Interestingly, it was shown that although the metastatic prostatic cancer cells express PSMA, only a few of the samples displayed neovasculature PSMA expression; the same is plausible for primary prostatic adenocarcinomas. However, the neovascular endothelial cells of metastatic clear cell renal carcinoma expressed PSMA in this study [75].

3.6.3.4 Serum

The expression of PSMA in serum is ambiguous. In some cases, GCPII was not detected in sera even from patients with actively progressive metastatic disease [66]. On the other hand, several studies report significant levels of PSMA in sera from prostate cancer patients;

moreover, serum PSMA levels in prostate cancer patients were found to be significantly higher than in normal controls [65; 67].

3.7 Alternatively spliced variants

Beside full-length GCPII, several other variants derived from the GCPII gene exist (Fig. 10). At first, so called PSM' was identified by RT-PCR of mRNA from normal prostate. PSM' has a shorter cDNA than PSMA, missing a 266-nucleotide region near the 5' end of PSMA cDNA (nucleotides 114-380). The deduced corresponding protein was 693 amino acids long. The missing region includes the translation initiation codon and codons for the transmembrane domain of PSMA; thus, the PSM' protein has no apparent signal sequence [76].

Later, PSM' protein was purified and sequenced. It was found that it lacks the first 59 amino acids of PSMA and displays molecular mass of 95 kDa (on SDS PAGE) [77].

In primary prostatic tumor, PSMA is the dominant form. In contrast, normal prostate expresses more PSM' than PSMA. Benign prostatic hypertrophy (BPH) samples showed about equal expression of both variants. The relative expression of PSMA and PSM' was called tumor index; LNCaP has the index ranging from 9 to 11, prostate carcinoma from 3 to 6, BPH from 0.75 to 1.6, and normal prostate from 0.075 to 0.45 [76].

O'Keefe *et al.* discovered two additional alternatively spliced variants of PSMA. The first, PSM-C, begins transcription at the same nucleotides as PSMA and PSM'. PSM-C contains the same splice donor site as PSM' (nt114) but uses an alternative splice acceptor site located within intron one of the PSMA gene. Transcription produces mRNA that contains additional 133 nucleotides compared to PSM'. However, PSM-C uses the same translation start codon as PSM' and would therefore produce a protein identical to PSM' [78].

PSM-D uses the same splice donor site as PSM' and a unique splice acceptor site located within intron one, introducing another novel exon. The putative translation of this protein shows a novel translation start codon within this new exon followed by 24 novel amino acids and the rest of the PSMA protein in frame [78]. Translation of PSM-D mRNA would produce a 97-kDa glycoprotein very similar to PSMA except for the presence of 2.5 kDa of different amino acids at the N-terminus. Since it would lack the transmembrane domain of PSMA, PSM-D protein should be localized intracellularly [79]. The expression of PSM-D mRNA was similar in normal prostate and primary prostate cancer, but was two-fold

higher in lymph node and bone metastases compared to the primary tumors. The expression of PSM-C did not differ within these categories [79].

The last variant described is termed PSM-E. PSM-E cDNA contains a new, 97-nucleotide exon inserted into PSM-E cDNA between nucleotide 379 and 380 of PSMA cDNA. On the other hand, a 93-nucleotide region (nucleotides 2,232–2,324 of PSMA cDNA) is deleted in PSM-E cDNA. Moreover, there are two different nucleotides between PSMA cDNA and PSM-E cDNA. The levels of PSM-E mRNA expression were significantly different among normal prostate, BPH, and prostate carcinoma, with the highest found for prostate cancer [80].

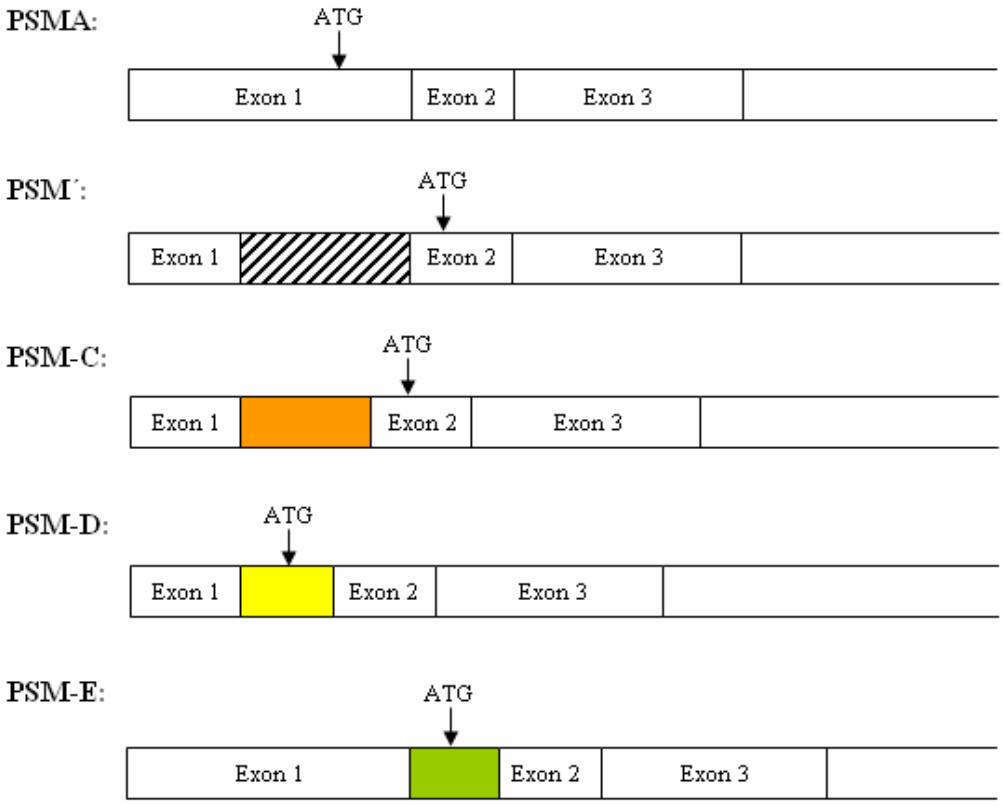

Fig. 10: Spliced variants derived from the GCPII gene. ATG, the translation start codon; crosshatched rectangle, the missing region in PSM´ compared to PSMA; orange rectangle, additional region in PSM-C compared to PSM´; yellow rectangle, additional exon in PSM-D compared to PSM´; green rectangle, a new exon in PSM-E.

3.8 Homologs of human GCPII

Beside the alternatively spliced variants that are all derived from the GCPII gene, several GCPII homologs have already been described. These include paralogs as well as orthologs of GCPII. Related genes and their encoded proteins that derive from a gene duplication event are paralogous; those that derive from speciation are orthologous. Proteins that are orthologous usually have a similar function [81].

3.8.1 Paralogs of human GCPII

3.8.1.1 Prostate Specific Membrane Antigen-Like gene (PSMA-L)

As to evolutionary distance, PSMA-L is the most closely related homolog of GCPII [82]. Deletion of the region corresponding to the promoter, exon 1, and a part of intron 1 of PSMA has been detected in the PSMA-like gene; moreover, the transcription of PSMA-L starts in the region corresponding to intron 5 of the PSMA gene. The longest open reading frame begins in the region corresponding to exon 8 of PSMA; thus, *in vitro* translation of the longest open reading frame yields a 46-kDa protein [83].

At the nucleotide level, the PSMA-like gene possesses 98% identity to the PSMA gene; the protein shows 97% identity to PSMA in the translated region [83]. However, due to a long deletion at the N-terminus, PSMA-L is not expected to be proteolytically active, since the removal of 90 amino acids from the N-terminus of PSMA already abolishes its hydrolyzing activity [84].

PSMA-L mRNA was found in liver and kidney [83].

3.8.1.2 Glutamate Carboxypeptidase III (GCPIII) / NAALADase II

GCPIII gene is localized in the same chromosome as GCPII, in the region 11q14.3, consists of 2223 bps and codes for the 740-amino acid protein. GCPIII was predicted to be a type II integral membrane protein containing a hydrophobic membrane spanning domain (amino acid residues 8–31) and possessing seven potential N-glycosylation sites. GCPII

protein sequence is 67% identical (81% similar) to that of GCPIII; COS cells transfected by GCPIII exhibited NAAG-hydrolyzing activity, although lower when compared to GCPII transfectants [64].

Northern blot analysis identified GCPIII mRNA in the largest amount in testis, ovary, and spleen; small amounts were also found in prostate, heart, placenta, intestine, pancreas, liver, kidney, and brain [64]. Consistently, Bacich *et al.* revealed second NAAG-hydrolyzing activity in brain of mice with a disrupted gene for GCPII [85].

The catalytic efficiency of purified recombinant human GCPIII was found to be comparable to that of GCPII as well as its susceptibility to 2-PMPA [26].

3.8.1.3 NAALADase L

Human NAALADase L mRNA was identified in 1997 in human ileum [86]. The full-length cDNA sequence comprises an open reading frame of 2223 bps encoding a protein consisting of 740 amino acids, with a calculated molecular mass of 80.6 kDa. It is predicted to be a type II membrane protein containing seven potential N-glycosylation sites. The predicted protein sequence is 35% identical (54% similar) to the sequence of GCPII. COS cells transfected with NAALADase L did not exhibit any NAAG-hydrolyzing activity. NAALADase L mRNA expression was highest in small intestine, spleen, and testis [64].

3.8.2 Orthologs of human GCPII

3.8.2.1 Rat GCPII

In the Robinson's pilot study, NAALADase activity was characterized for the first time. GCPII bound in the rat brain membranes cleaved NAAG with K_m=540 nM and this activity was sensitive to phosphate, EDTA, and quisqualate [1]. Purified rat GCPII displayed even lower K_m value - 140 nM - and migrated as a 94-kDa band [87].

Rat GCPII cDNA possesses 83% homology with the human GCPII gene. The predicted 752-amino acid sequence has 85% identity and 91 % similarity to the human GCPII sequence. Nine potential N-glycosylation sites were deduced to reside in the extracellular domain. Cells

transfected with rat GCPII DNA exhibited NAAG-hydrolyzing activity, which was inhibited by quisqualate [88].

In rat, pronounced GCPII activity was revealed in brain and kidney; low to negligible NAAG-hydrolyzing activity was measured also in adrenal gland, lung, heart, liver, small intestine, pancreas, testis, and skeletal muscle [1]. GCPII mRNA was found in rat brain, kidney, and spinal cord [88; 27]. Western blotting identified GCPII protein in rat brain, kidney, and testis [87]. However, GCPII was not detected in the rat prostate.

3.8.2.2 Murine GCPII

The 2,256-nt open reading frame of mouse GCPII gene encodes for a 752-amino acid protein, with 86% identity and 91% similarity to the human GCPII amino acid sequence. The predicted type II membrane protein possesses 10 potential N-glycosylation sites. Transfected cells gained both NAALADase and folate hydrolase activities [89].

Pronounced expression of mouse GCPII mRNA and NAAG-hydrolyzing activity were found in brain and kidney; faint signal was detected also in salivary gland, ovary, and testis. While several studies could not find any significant amount of GCPII mRNA in murine prostate, Yang *et al.* observed GCPII mRNA positivity in there [89; 90; 91].

3.8.2.3 Porcine GCPII

Porcine GCPII consists of 751 amino acids, shares 91% amino acid sequence identity to human GCPII and harbors 12 potential N-glycosylation sites. PC3 transfectant membranes exhibited activities of folylpoly-γ-carboxypeptidase and NAALADase; NAALADase activity was 16-fold greater in porcine jejunal brush-border membranes than in ileal brush-border membranes. Porcine GCPII mRNA was found in duodenal and jejunal mucosa and in a lesser amount in kidney [51].

3.9 GCPII as a therapeutic target

3.9.1 GCPII in neuropathies

3.9.1.1 Excitotoxicity

At the resting membrane potentials, Mg^{2+} ions occupy the ion channel of the NMDA receptor to prevent Ca^{2+} influx. This blockade is voltage-dependent and hence removed by depolarization [92]. Failure to maintain the membrane potential caused by prolonged depolarization associated with excessive glutamate release might trigger an excitotoxic cascade, especially through the activation of Ca^{2+}-dependent processes [93; 94]. NMDA receptors are permeable for Na^{+} ions, too, that can also damage neurons. In addition, metabotropic glutamate receptors mediate the cascade of events that causes mobilization of Ca^{2+} from internal stores [95].

It seems that excitotoxicity is made up of two components. The first is an acute, Na^{+} and Cl^{-} dependent component, which is marked by immediate cell swelling. The second component is Ca^{2+}-dependent delayed cell degeneration [96]. Ca^{2+} overload can trigger many neurotoxic cascades, including uncoupling the mitochondrial electron transfer from ATP synthesis, activation and overstimulation of enzymes such as calpains and other proteases, protein kinases, nitric oxide synthase, calcineurins, and endonucleases. Alterations in activity of these enzymes can lead to: (i) increased production of toxic reactive oxygen species such as nitric oxide, superoxide, and hydrogen peroxide; (ii) alterations in the organization of the cytoskeleton; (iii) activation of genetic signals leading to cell death (apoptosis); and (iv) mitochondrial dysfunction [95].

In an agreement with these findings, it was shown that neurons in culture can be killed if they are bathed in as little as 10–40 μM glutamate, despite the fact that the average glutamate intracellular concentration in the mature human brain is over 11 mM [97; 98].

As cleaving NAAG and thus increasing glutamate levels and also simultaneously decreasing NAAG levels, GCPII can influence pathologic processes in the nervous system (given the glutamate-mediated excitotoxicity as well as NAAG action: suppression of the glutamate release via presynaptic mGluRs and activation of mGluR3 on glial cells leading to secretion of neuroprotective TGF-β – see above).

3.9.1.2 Ischemia and stroke

The extremely low intraneuronal levels (approximately 100 nM) of Ca^{2+} are maintained through the: (1) entry of extracellular Ca^{2+} through ligand-operated receptors or voltage-gated Ca^{2+} channels; (2) release of Ca^{2+} from the endoplasmic reticulum through the stimulation of inositol 1,4,5-trisphosphate receptors, or from the mitochondria through the Na^{+}-Ca^{2+} exchanger; (3) extrusion of Ca^{2+} through the Ca^{2+}-ATPase or Na^{+}-Ca^{2+} exchanger in the plasma membrane (4); binding of Ca^{2+} to target proteins; (5) sequestration of Ca^{2+} into the endoplasmic reticulum through Ca^{2+}-ATPase, or mitochondria through electrophoretic (uniport) mechanisms [99; 100; 101]. Thus, energy failure in hypoxic ischemia will cause the accumulation of intraneuronal Ca^{2+} by enhancing the entry and release of Ca^{2+}, and interfering with the ATP-dependent extrusion and sequestration of Ca^{2+} (Fig. 11, 12). The entry of Ca^{2+} through NMDA receptors appears to underlie a major portion of the Ca^{2+} overload following hypoxic ischemia [102].

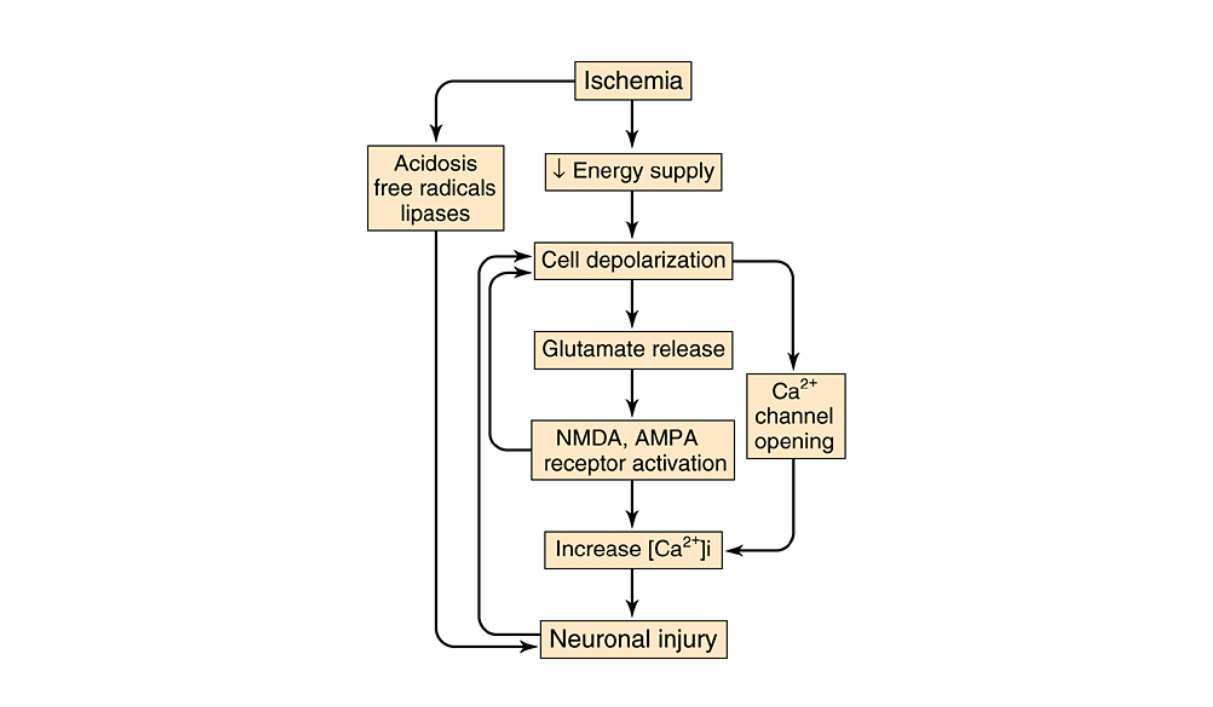

Fig. 11: Complex scheme of potential paths leading to neuronal injury resulting from an ischemic episode. Ischemia-induced events involve the depletion of cellular energy stores and the release of free radicals. The energy depletion permits sustained activation of glutamate receptors and entry of Ca^{2+} via NMDA receptors, AMPA receptors, and voltage-gated Ca^{2+} channels. Elevation of intracellular Ca^{2+} causes massive activation of a variety of Ca^{2+}-dependent enzymes. Taken from [105].

Slusher *et al.* showed that the GCPII inhibitor 2-PMPA robustly protects against ischemic injury in a neuronal culture model of stroke and in rats after transient middle cerebral artery occlusion (MCAO), simultaneously increasing NAAG levels and attenuating the ischemia-induced rise in glutamate [103].

GCPII inhibitor GPI5232 ([2-[(pentafluorophenylmethyl)hydroxyphosphinyl]methyl)-pentanedioic acid]) was found not only to decrease brain injury but also to alter the inherent electroencephalographic changes observed in a rat model of transient middle cerebral artery occlusion. MCAO-injured rats were also predisposed to developing cortical seizures and GPI5232-treated rats had significantly fewer seizures [104].

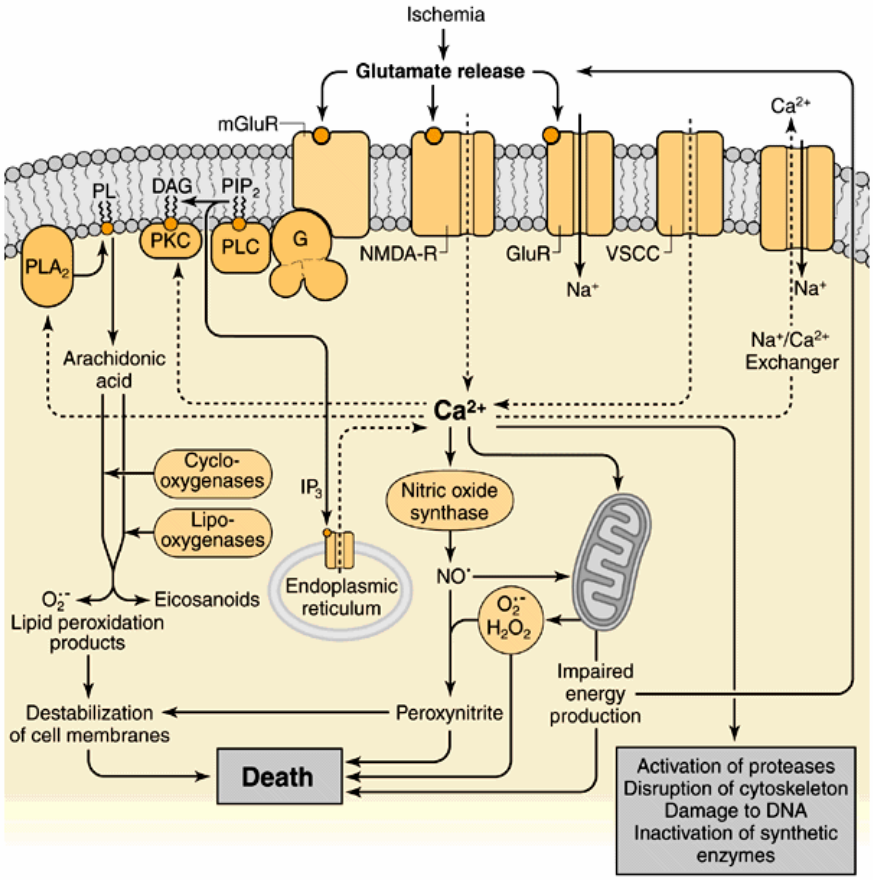

Fig. 12: Particular mechanisms contributing to neuronal injury during ischemia. mGluR, metabotropic glutamate receptor; NMDA-R, N-methyl-D-aspartate receptor; GluR, AMPA/kainate type of glutamate receptors; PL, phospholipids; PLA_2, phospholipase A_2; DAG, diacylglycerol; PLC, phospholipase C; PKC, protein kinase C; G, G protein; PIP_2, phosphatidylinositol 4,5-bisphosphate; IP_3, inositol 1,4,5-trisphosphate; $NO^{\bullet}$, nitric oxide; $O_2^{\bullet -}$, superoxide radical; H_2O_2, hydrogen peroxide; VSCC, voltage-sensitive Ca^{2+} channel. Taken from [105].

3.9.1.3 Neuropathic and inflammatory pain

Pain is caused by an injury to the peripheral or central nervous system. Increased glutamate availability in the spinal cord and primary afferent neurons is important in acute and chronic pain [50].

2-PMPA and urea-based GCPII inhibitors reduce perception of neuropathic and inflammatory pain in rat models [106; 107; 108]. The analgesic effect of the latter was blocked by pretreatment with group II mGluRs antagonist [108], which suggests that the GCPII inhibitors produce analgesia by elevating the extracellular NAAG levels and thus activating group II mGluRs [50].

3.9.1.4 Chronic neurodegenerative diseases

Elevated GCPII activity was described in certain regions of brain of genetically epilepsy-prone rats [109].

Passani *et al*. reported that decreases in the levels of NAAG and NAA and in the activity of GCPII in Alzheimer's and Huntington's brain correlate primarily with neuronal loss [110].

Levels of NAAG were increased and GCPII activity and glutamate levels were decreased in the schizophrenic brains [111].

In amyotrophic lateral sclerosis (ALS), selective regional reductions in NAA and NAAG (in addition to that of glutamate and aspartate) were reported in the central nervous system, whereas the activity of GCPII was increased [112]. It was shown that inhibition of GCPII by 2-PMPA *(in vitro)* and 2-MPPA *(in vivo)* protects motor neurons from death in familial amyotrophic lateral sclerosis models [113].

However, the contribution (if any) of GCPII to the development of these diseases still remains to be elucidated.

3.9.2 GCPII as a target in cancer treatment/diagnosis

GCPII represents a target for prostate cancer diagnosis and therapy because of its membrane localization and highly upregulated expression in prostate carcinoma (with the greatest extent and intensity of GCPII staining observed in the highest grades) [71; 114].

3.9.2.1 GCPII as a diagnostic marker

3.9.2.1.1 Anti-GCPII antibodies

ProstaScint (Capromab pendetide) is an ^{111}In-labeled immunoconjugate of anti-GCPII monoclonal antibody 7E11-C5.3 [115]. It is currently used as a radioimmunoscintigraphic imaging agent capable of detection of prostate cancer and/or its metastases *in vivo* [116; 117; 118] (in 1997, it was approved by the FDA for usage in human medicine). Unfortunately, the epitope of the 7E11-C5.3 antibody is localized in the intracellular part of GCPII; thus, some believe that this antibody is capable of imaging only cells that are dead or dying [119]. That is why antibodies recognizing extracellular epitope of GCPII are being sought and evaluated as potential imaging agents [120; 121].

3.9.2.1.2 Small GCPII ligands

In 2003, Tang *et al.* synthesized nine phosphonate/phosphinate-based GCPII inhibitors, mimicking the tetrahedral transition state of NAAG hydrolysis, all displaying IC_{50} value of 120 nM or lower (to LNCaP-membrane-associated GCPII). The most efficient of them, VA-033C, inhibits GCPII with the IC_{50} value of 12.5 nM, which is not substantially altered by fluorescent modification. Other two inhibitors of this series, fluorescently labeled, were shown to bind to membranes of viable LNCaP cells. None of the compounds alters the cell cycle kinetics or induces apoptosis in LNCaP cells [122].

Later, radiolabeled urea-based GCPII ligands with the K_i value of 1.5 and 1.9 nM, respectively, were shown to bind preferentially to LNCaP-derived xenografts *in vivo* (as compared to GCPII-negative PC3 cells and breast-cancer-derived xenografts) [123].

High-affinity fluorescent agents for *in vivo* imaging of GCPII were also described [124].

3.9.2.2 GCPII as a therapeutic target in cancer

Various approaches of GCPII-based cancer treatment have been described.

Most of the therapeutic strategies currently tested are based on modified components of the immune system. Several reports document using dendritic cells pulsed with GCPII-derived peptides possessing a high affinity for MHC class I that stimulate an autologous cytotoxic T-cell response [125; 126; 127]. About 30% of study participants showed a positive response at the conclusion of the phase II trial [127]. However, tumor escape by down-regulation of target antigens may limit the susceptibility of tumor cells to the attack. Therefore, the immunostimulatory capacity of autologous dendritic cells pulsed with multiple T cell epitopes derived from four different prostate-specific proteins (prostate stem cell antigen, prostatic acid phosphatase, PSMA, and prostate-specific antigen) was determined; vaccination elicited significant cytotoxic T cell responses against all the antigens tested [128].

Other approach exploits anti-GCPII antibodies either conjugated to toxins or radiolabeled by ^{90}Yttrium or ^{177}Lutecium. Treatment with monoclonal anti-GCPII antibody J591 conjugated to ricin A-chain resulted in complete eradication of 3-D tumor micromasses of LNCaP cells or in reduction of target cells number, depending on the dose [129]. The same antibody radiolabeled by ^{90}Yttrium or ^{177}Lutecium accurately targeted bone and/or soft tissue lesions [130; 131].

Human primary T lymphocytes expressing artificial fusion receptors comprising an antibody fragment recognizing GCPII, T-cell receptor-ζ, and CD28 signaling elements effectively lyse tumor cells expressing PSMA [132].

Other then immunological strategies are also being developed. Since the genes under the control of the GCPII promoter/enhancer were shown to be much more active in prostatic cell lines than in several others, construct comprising *E. coli* cytosine deaminase gene under the regulatory control of the GCPII promoter/enhancer was used to convert the nontoxic prodrug 5-fluorocytosine into the cytotoxic compound 5-fluorouracil in prostate cancer cells. Tumors of mice bearing this construct were significantly reduced following 5-fluorocytosine treatment [133; 134].

4 AIMS OF THE STUDY

In an attempt to help to identify a suitable animal model for *in vitro* and *in vivo* studies concerning novel GCPII-based diagnostic/therapeutic approaches, we aimed to:

- kinetically characterize rat and pig orthologs of human GCPII in terms of K_m, k_{cat}, and susceptibility to the inhibitor 2-PMPA;
- map the expression pattern of GCPII in a panel of human, rat, and porcine tissues using immunochemistry detection with a sensitive monoclonal antibody GCP-04;
- confirm the observed expression pattern by activity measurements in the tissue samples.

To broaden the knowledge of ligand binding and cleavage by GCPII and thus help to design GCPII ligands with more convenient pharmacokinetic and pharmacodynamic parameters, we decided to:

- map the enzyme-substrate interactions in the S1' pocket of GCPII on the basis of crystal structure analysis and kinetic measurements;
- map the enzyme-substrate interactions in the S1 pocket of GCPII (by the same way).

5 LIST OF PUBLICATIONS

Publications included in the thesis:

- Rovenská, M., Hlouchová, K., Šácha, P., Mlčochová, P., Horák, V., Zámečník, J., Bařinka, C., Konvalinka, J. Tissue Expression and Enzymologic Characterization of Human Prostate Specific Membrane Antigen and Its Rat and Pig Orthologs. Prostate 2008; 68: 171-82.

- Bařinka, C., Rovenská, M., Mlčochová, P., Hlouchová, K., Plechanovová, A., Majer, P., Tsukamoto, T., Slusher, B.S., Konvalinka, J., Lubkowski, J. Structural Insight into the Pharmacophore Pocket of Human Glutamate Carboxypeptidase II. J. Med. Chem. 2007; 50: 3267-3273.

- Barinka, C., Hlouchova, K., Rovenska, M., Majer, P., Dauter, M., Hin, N., Ko, YS., Tsukamoto, T., Slusher, B.S., Konvalinka, J., Lubkowski, J. Structural Basis of Interactions between Human Glutamate Carboxypeptidase II and Its Substrate Analogs. J. Mol. Biol. 2008; 376: 1438-50.

Publication not included in the thesis:

- Nijhuis, M., van Maarseveen, N.M., Lastere, S., Schipper, P., Coakley, E., Glass, B., Rovenska, M., de Jong, D., Chappey, C., Goedegebuure, I.W., Heilek-Snyder, G., Dulude, D., Cammack, N., Brakier-Gingras, L., Konvalinka, J., Parkin, N., Kräusslich, HG., Brun-Vezinet, F., Boucher, C.A. A Novel Substrate-based HIV-1 Protease Inhibitor Drug Resistance Mechanism. PLoS Med. 2007; 4: 0152-0163.

6 RESULTS

6.1 Publication I:

Tissue Expression and Enzymologic Characterization of Human Prostate Specific Membrane Antigen and Its Rat and Pig Orthologs

Background:

GCPII is a potential target for diagnosis and treatment of prostate cancer and, moreover, for a generation of novel antineoplastics due to its upregulation in the vasculature of most solid tumors. For corresponding studies, a suitable animal model is needed. Since rat and pig GCPII display very high amino acid sequence identity to human GCPII (85% and 91%, respectively), we decided to recombinantly produce rat and pig orthologs of human GCPII and characterize them in terms of K_m, k_{cat}, and susceptibility to the inhibitor 2-PMPA. In addition, we investigated the expression pattern of GCPII in a panel of human, rat, and porcine tissues - up to now, this has not been done in one consistent study and findings acquired by different methods did not allow for making comparisons. Presence of GCPII in selected tissues was further confirmed by activity measurement and in three cases also by immunohistochemistry.

Comments:

We prepared extracellular parts of GCPII of *Homo sapiens sapiens* (hGCPII), *Rattus norvegicus* (rGCPII), and *Sus scrofa* (pGCPII) by recombinant expression in *Drosophila* S2 cells. For rGCPII and pGCPII in conditioned media and for purified hGCPII, we radioenzymatically determined the values of K_m and k_{cat} for NAAG cleavage and IC_{50} for 2-PMPA. We found out that the catalytic efficiencies (k_{cat}/K_m) of all three orthologs are very similar; the values of IC_{50} also do not differ very much (IC_{50} for hGCPII is slightly higher than for the other two orthologs).

GCPII expression was examined by Western blotting and subsequent immunodetection using the monoclonal antibody GCP-04 in human, rat, and pig brain, spinal cord, spleen, lung, mammary gland, heart, stomach, liver, pancreas, kidney, jejunum, ileum, colon, urinary

bladder, ovary, uterus, prostate, testes, skeletal muscle, skin, and fat. Generally, it was shown that GCPII tissue distribution is diverse in the three species. Only brain and kidney displayed rich GCPII expression in all three species; moderate to high GCPII expression was observed also in human spinal cord, spleen, lung, liver, jejunum, ileum, ovary, and prostate; in rat spinal cord and testes; and in pig spinal cord, spleen, lung, mammary gland, heart, stomach, liver, jejunum, ileum, large intestine, urinary bladder, ovary, uterus, testes, skeletal muscle, and fat. Thus, GCPII is most abundantly expressed in pig tissues, while its expression in rat is the most restricted. In human, GCPII expression is definitely not prostate-specific, as it was formerly thought. Interestingly, although we confirmed high level of GCPII in human prostate, rat and pig prostates show very low GCPII expression.

To confirm and complement these findings, we measured NAAG-hydrolyzing activity in human, rat, and pig brain, prostate, urinary bladder, skin, heart, and skeletal muscle; and in human and pig fat; and in pig jejunum, kidney, and testes. The activities normalized for total protein concentration roughly correlated with the intensities observed on Western blots.

Because of the high sequence similarity, not only hGCPII, but also its close homologs could be detected by the GCP-04 antibody. We showed that GCP-04 recognizes hGCPII, rGCPII, and pGCPII with a similar sensitivity. We also found that the GCP-04 antibody crossreacts with recombinant extracellular part of human GCPIII, with an approximately two-order-of-magnitude lower sensitivity than for hGCPII. In analogy, the activity measured in tissue homogenates could be a superposition of activities of GCPII and its various homologs. We have measured that the activity of recombinant extracellular part of human GCPIII is approximately three times lower than activity of hGCPII in conditions used in this study.

Based on our kinetic data, it seems that rat and pig GCPII could be suitable to approximate the human enzyme in kinetic measurements *in vitro*. On the other hand, the different tissue distribution of GCPII in the three species must be taken into account when using rat of pig as models for *in vivo* studies. Moreover, the widespread expression of GCPII in human may represent a potential caveat for the utility of GCPII-targeted anti-cancer compounds.

My contribution:

I performed all the kinetic measurements and immunochemistry analyses.